Chin. Phys. Lett. **39**, 033401 (2022)

High Energy Inner Shell Photoelectron Diffraction in CO_2

Xiaohong Li(李晓红)[1,2], Bocheng Ding(丁伯承)[1,2], Yunfei Feng(封云飞)[1,2], Ruichang Wu(吴睿昌)[1,2], Lifang Tian(田莉芳)[1,2], Jianye Huang(黄健业)[1,2], and Xiaojing Liu(刘小井)[1,2*]

[1]*School of Physical Science and Technology, ShanghaiTech University, Shanghai 201210, China*
[2]*Center for Transformative Science, ShanghaiTech University, Shanghai 201210, China*

(Received 29 November 2021; accepted 13 February 2022; published online 1 March 2022)

Photoelectron diffraction is an effective tool to probe the structures of molecules. The higher the photoelectron kinetic energy is, the higher order the diffraction pattern is disclosed in. Up to date, either the multi-atomic molecule with the photoelectron kinetic energy below 150 eV or the diatomic molecule with 735 eV photoelectron has been experimentally reported. In this study, we measured the diffraction pattern of C 1*s* and O 1*s* photoelectrons in CO_2 with 319.7 and 433.5 eV kinetic energies, respectively. The extracted C–O bond lengths are longer than the C–O bond length at the ground state, which is attributed to the asymmetric fragmentation that preferentially occurs at the longer chemical bond side during the zero-energy asymmetric vibration.

DOI: 10.1088/0256-307X/39/3/033401

Researchers struggle to follow and control chemical reactions in real time, so-called "molecular movie". There are two essential factors: time and spatial resolutions. The femtosecond and free-electron lasers bring the time resolution to reality; however, the tool to image the molecular structure still needs to be enriched. The methods for measuring the molecular structure include ultrafast electron diffraction,[1] femtosecond time-resolved electron microscopy,[2] ultrafast x-ray diffraction,[3] high-order harmonics spectrum ,[4] Coulomb explosion,[5] laser-induced electron diffraction.[6] Yang *et al.*[1] used ultrafast electron diffraction to measure the CF_3I molecular deformation with the spatio-temporal resolution of 80 fs/0.01 Å. Wang *et al.*[2] measured carrier dynamics of single-layer WSe_2 using femtosecond time-resolved photoemission electron microscopy with 60 fs/80 nm resolution. Glownia *et al.*[3] measured the change in the I_2 bond length at the spatio-temporal resolution of 30 fs/0.3 Å using x-ray diffraction method. The highest occupied orbital wave function density of diatomic molecules can be obtained from the high-order harmonic spectrum with the molecules aligned.[4] Coulomb explosion can give the instantaneous internuclear distance.[5] Wolter *et al.*[6] measured the change in the C_2H_2 bond length with a resolution of 0.6 fs/0.15 Å using laser-induced electron diffraction. Generally, these methods have their characteristics and complement each other. Photoelectron diffraction is also an important technique.

The molecular frame photoelectron angular distribution (MFPAD)[7–15] and the electron frame photoion angular distribution (EFPAD)[16] are used to describe the electron emission in its intrinsic frame. At the kinetic energy lower than 30 eV, MFPAD or EFPAD can be described by propagating the spherical harmonic partial waves in the molecular Coulomb potential. For the kinetic energy above 100 eV, MFPAD and EFPAD can be interpreted by x-ray photoelectron diffraction.

Photoelectron diffraction is an approach that images molecules from within.[17] The electron wave is emitted from a specific element with the incident photon energy above the core ionization threshold and scattered by the neighboring atoms before it escapes from the molecule. The direct and scattered waves are coherently superimposed in space to form a diffraction pattern. The molecular structure can be extracted from the diffraction pattern.

Furthermore, photoelectron diffraction is relatively mature in detecting geometric structures of solids and surfaces,[18,19] as well as in the molecules absorbed on the surface.[20,21] It can also detect the structure of gas-phase molecules. Most previous studies have focused on diatomic molecules.[12,22–25] In particular, Grundmann *et al.*[24] measured the photoelectron diffraction pattern in H_2 with a photoelectron energy of 735 ± 15 eV, and the pattern is clear enough to reveal phase changes in the electron emission. It is also essential to extend photoelectron diffraction to multi-atomic molecules. Most recently, Tsuru *et al.*[14,26] observed the angular distribution of photoelectrons of C 1*s* and O 1*s* in CO_2, with the photoelectron energy of about 150 eV. Here, the first maxima in the diffraction pattern are only barely resolved due to the limited electron kinetic energy. Thus, it is essential to

*Corresponding author. Email: liuxj@shanghaitech.edu.cn
© 2022 Chinese Physical Society and IOP Publishing Ltd

observe more maxima in the diffraction pattern with higher kinetic energy.

In this Letter, we measured the C 1s and O 1s photoelectron diffraction pattern in the CO_2 molecule and extended the electron kinetic energy to 319.7 and 433.5 eV, respectively. We also tried to verify how photoelectron diffraction can be used to extract the ground state structure of gas-phase polyatomic molecules.

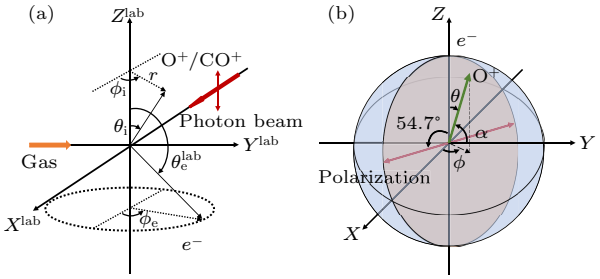

Fig. 1. Definition of (a) the lab frame and (b) the electron frame. In (a) the lab frame, the light propagation is perpendicular to the gas beam. The polarization of the light is vertical. Electrons are collected within the polar angle of 54° ± 3°, and ions are collected in 100% of 4π sr. In (b) the electron frame, the Z-axis is defined by the electron emission direction. The Y-axis is defined by the cross-product of the Z-axis and polarization direction, and the X-axis is defined according to the right-hand rule. Here, θ and ϕ are the polar and azimuth angles, respectively; α is the angle between the O^+ and Y-axis used to define the thickness of the layer parallel to the ZX plane, i.e., the degree of the coplanar. The layer is defined by $85° < \alpha < 95°$.

The experimental method has been described in Ref. [27]. We only give a brief description here. The experiments were conducted using the EPICEA setup at the PLEIADES beamline[28] at Synchrotron SOLEIL in France. The EPICEA setup consists of a double-toroidal electron analyzer (DTA)[29–31] and an ion time of flight (TOF) spectrometer.

As shown in Fig. 1(a), the light polarization is vertical in the lab frame. DTA selects the electrons within the polar angle of $54 \pm 3°$ and the entire 2π azimuthal angle with respect to the vertical axis. DTA was operated around the central kinetic energy of 319.7 and 433.5 eV with the pass energies of 180 and 300 eV, respectively. Here, the photoelectron kinetic energy value is selected to avoid overlap from the Auger electron and to keep the reasonable ionization cross-section. The energy resolution of the electron is around 0.8% of the pass energy.

The ion TOF spectrometer with a position-sensitive detector was mounted opposite the DTA, which can measure the ion momentum. A pulsed voltage was triggered by the detection of the photoelectron and pushed ions toward the ion detector. The mass resolution for zero kinetic-energy ion was ∼1000. The ion momentum and energy resolutions were ∼1.4 a.u. and ∼0.3 eV, respectively. We used a random signal generator to simulate false coincidence events and subtracted the contribution of false coincidence events from the data according to the method described by Prümper *et al.*[32]

Next, O^+/CO^+ pair is produced after C 1s and O 1s ionization and Auger electron emission. The ionization and Auger processes can be written as

$$\begin{aligned} CO_2 + h\nu \rightarrow & CO_2^+ + e_{\rm ph}^- \\ \rightarrow & O^+ + CO^+ + e_{\rm ph}^- + e_{\rm Aug}^-, \end{aligned}$$

where $e_{\rm ph}^-$ is the photoelectron, and $e_{\rm Aug}^-$ is the Auger electron. We used O^+ from the O^+/CO^+ pair to define the molecular axis. Since the polar angle between the electron and polarization is fixed in our experiment, we used EFPAD[16] to describe the reaction, as shown in Fig. 1(b). We retrieved EFPADs with two methods under the electron frame. The first approach is the layer-selection method. The events are selected within the layer that the three directions (light polarization, electron emission, and ion fragment) are coplanar within ±5°. The second approach is the projection method,[13] where the EFPAD is expressed by four $F_{LN}^{(e)}(\theta)$ functions[16]

$$\begin{aligned} I(\theta,\phi,[\theta_{\rm e}^{\rm lab}]) = & F_{00}^{(e)}(\theta) + F_{20}^{(e)}(\theta) P_2^0(\cos[\theta_{\rm e}^{\rm lab}]) \\ & + F_{21}^{(e)}(\theta) P_2^1(\cos[\theta_{\rm e}^{\rm lab}])\cos\phi \\ & + F_{22}^{(e)}(\theta) P_2^2(\cos[\theta_{\rm e}^{\rm lab}])\cos(2\phi). \quad (1) \end{aligned}$$

Here, P_L^N is the Legendre polynomial. All information about ion distribution is contained in these four $F_{LN}^{(e)}(\theta)$ functions. After four $F_{LN}^{(e)}(\theta)$ functions are retrieved by the projection of all events, the one-dimensional (1D) differential cross-section $I(\theta,\phi,[\theta_{\rm e}^{\rm lab}])|_{\theta_{\rm e}^{\rm lab}=54.7°}^{\phi=0° \text{ or } 180°}$ is calculated.

Figures 2(a) and 2(b) show the EFPAD of C 1s using the layer-selection and projection methods, respectively. We observed periodically modulated diffraction patterns in both cases. It can be seen that the lobars and nodals are consistent with these two patterns, except for the intensity scale. Although the shape of these two patterns should be the same in principle, a few marginal differences are observed. These differences can be attributed to the inhomogeneous detection efficiency of the position-sensitive detector, which can be as large as 15%. The projection method uses all events, whereas the layer-selection method uses only part of the events. Therefore, the intensity scale is different. The EFPAD of C 1s in Fig. 2(a) is almost symmetric with respect to the reflection plane of symmetry. The core hole is located in the center of the molecule after C 1s photoelectrons are emitted, inducing a symmetrical potential. Thus, the symmetric vibration dominates[33] and results in symmetric EFPAD.

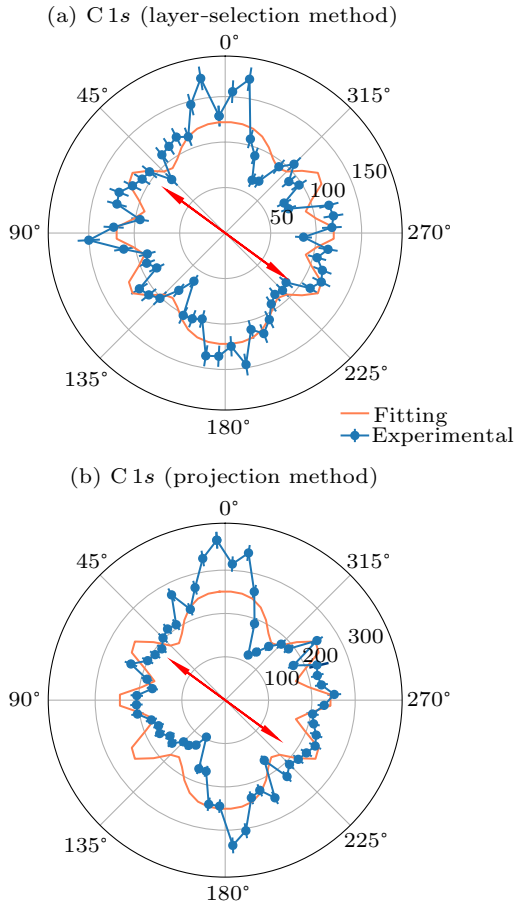

Fig. 2. The EFPAD from C 1s photoionization using (a) the layer-selection method and (b) the projection method. The blue-filled circle shows the experimental data, and the solid orange line shows the results fitted by Eq. (2). The double arrow represents the polarization. The electron emission direction defines 0°. The angular direction is counterclockwise and consistent with Fig. 1(b).

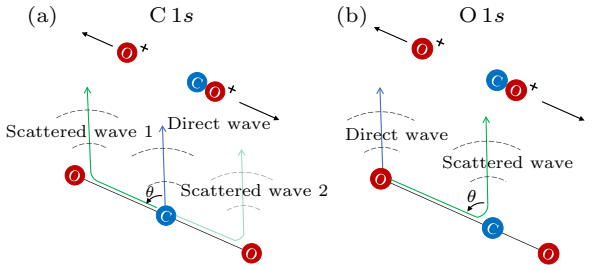

Fig. 3. Diffraction mechanism in (a) C 1s and (b) O 1s photoionization from the CO_2 molecule.

Figure 3(a) shows the diffraction mechanism of C 1s photoionization in the CO_2 molecule. After releasing the photoelectron, the electron wave can be directly released or scattered by the two neighboring O atoms. Here, with the kinetic energy above 300 eV, the photoelectron can easily penetrate through the valance and inner valance orbitals and be scattered by the Coulomb potential of the nuclear and 1s orbital, so the scattering sites can be treated as geometry points. The direct and two scattered waves are superimposed in space. By assuming that the direct and scattered are spherical waves, the diffraction pattern as a function of the angle between photoelectron and O^+ fragments is written as

$$\begin{aligned} I =& A^2 + 2B^2 + 2AB\cos(\phi_{\rm L}) \\ &+ 2AB\cos(\phi_{\rm R}) + 2B^2\cos(\phi_{\rm L} - \phi_{\rm R}), \end{aligned} \tag{2}$$

where A is the amplitude of the direct wave; B is the amplitude of the scattered wave. The phase differences between the direct and scattered waves are given as follows:

$$\phi_{\rm L} = 2\pi R\frac{(1-\cos\theta)}{\lambda}, \tag{3}$$

$$\phi_{\rm R} = 2\pi R\frac{(1+\cos\theta)}{\lambda}. \tag{4}$$

Here, R is the C-O bond length; λ is the de Broglie wavelength of the photoelectron. The experimental data are fitted with this function, which is represented by the solid orange line in Fig. 2. The lobars and nodals are consistent with the experimental results. The agreement in intensity is not so good because of the model's simplicity. For example, it is known that the direct wave should be the p-type; however, the waves are simply assumed as spherical in the model. Furthermore, the data are analyzed in the electron frame instead of the conventional molecular frame, which would change the intensity of the diffraction pattern. Moreover, the positions of the lobars and nodals should not change; thus, we can still extract the C–O bond length from this fitting. Table 1 presents the values of fitting parameters. The extracted C–O bond lengths using the layer-selection and projection methods are 1.34 ± 0.03 Å and 1.35 ± 0.04 Å, respectively. They are longer than the bond length of the ground state (1.16 Å). This is because the zero-energy asymmetric vibration persists. Although the averaged left C–O bond length equals the averaged right C–O bond length, the instantaneous left C–O bond length can be different from the instantaneous right C–O bond length at the moment of the photoionization. Furthermore, the dissociation bond is always longer during the zero-energy asymmetric vibration.[34] Thus, the extracted bond length is longer than that at the ground state. Since these two analysis methods are consistent, we only present the result using the layer-selection method.

Figure 4(a) shows the EFPAD at O 1s in the CO_2 molecule. The O 1s diffraction pattern is strongly asymmetric than the C 1s diffraction pattern. Two steps in the mechanism must be considered. During ionization, the antisymmetric stretching mode is triggered.[35,36] The O 1s core-hole lifetime width $\Gamma = 163$ meV, and the corresponding lifetime $\delta t = 2$ fs. The antisymmetric vibrational energy interval

$\hbar\omega = 307\,\text{meV}$,[37] and the corresponding vibration period $T = 13.5\,\text{fs}$. Here, $\delta t < T/4$ means that the molecule shifts from the original symmetric structure to its new asymmetric equilibrium structure during the O 1s core-hole lifetime. Assuming photoionization occurs at the left O atom, the left C–O bond starts to be irreversibly elongated and causes asymmetry in the angular distribution. If the Auger final state is predissociative with a relatively long timescale, the molecular dication can return to a symmetric structure, and MFPAD may become symmetric again.[9] If the Auger final state is directly dissociative and fragments rapidly, the asymmetry in the angular distribution remains. Thus, EFPAD includes these two kinds of contributions.

Table 1. The parameters obtained by fitting. A: amplitude of the direct wave, B: amplitude of the scattered wave.

	C 1s (layer-selection method)	C 1s (projection method)	O 1s (layer-selection method)
R (Å)	1.34 ± 0.03	1.35 ± 0.04	1.34 ± 0.05
A	10.26 ± 0.12	14.34 ± 0.23	8.35 ± 0.10
B	0.56 ± 0.09	0.77 ± 0.17	0.36 ± 0.13

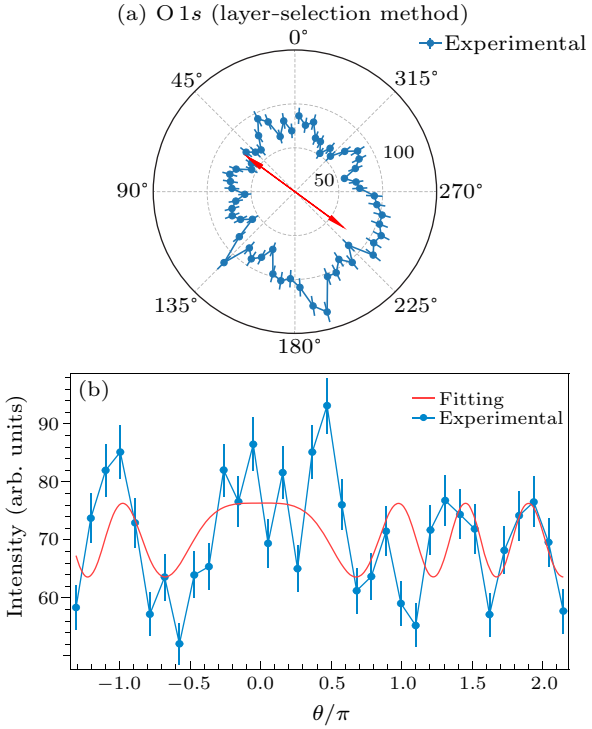

Fig. 4. (a) EFPAD from O 1s photoionization using the layer-selection method. (b) The top half of the EFPAD is represented in rectangular coordinate.

Tsuru *et al.*[26] obtained that the intensity increases in the forward direction as the photoelectrons' energy increases from 85 to 150 eV. This is consistent with our observation that the photoelectron is emitted from the O side and tends to be enhanced at the direction of its partner CO^+ at the kinetic energy of 433.5 eV, called forward focusing in scattering theory.

Figure 3(b) shows the mechanism of the O 1s photoelectron diffraction to obtain the molecular structure in this case. When O 1s photoelectron is released from the left O atom, the photoelectron can be scattered by the C atom. The scattering cross-section on the nonneighbor O atom is neglected because it is smaller than that on the neighbor C atom. Thus, the formula is given as follows:

$$I = A^2 + B^2 + 2AB\cos(\phi), \tag{5}$$

$$\phi = 2\pi R\frac{(1-\cos\theta)}{\lambda}. \tag{6}$$

The photoelectron is forward-focused by the C atom; thus, the bottom half of the diffraction pattern in Fig. 4(a) is distorted. However, the backward scattered photoelectrons on the top half of Fig. 4(a) are not affected and still show the characteristics of photoelectron diffraction. Thus, we choose the top half data in Fig. 4(a) and show the EFPAD in a rectangular coordinate in Fig. 4(b). Then, the data are fitted with Eqs. (5) and (6).

The orange line in Fig. 4(b) shows the fitted result. The lobars and nodals of the fitting and experimental results are also consistent. Table 1 presents the parameters obtained by fitting. Here, the C–O bond length is 1.34 ± 0.05 Å. It seems strange that this value is the same as those measured at C 1s but can be understood because photoelectron emission occurs within several tens of attoseconds, during which the molecular structure does not change much. However, the coherence between two O atoms is already destroyed in the case of O 1s ionization.

To summarize, we have measured the diffraction patterns in the form of EFPAD with the photoelectron energies of 319.7 and 433.5 eV above C 1s and O 1s thresholds of CO_2, respectively. The diffraction pattern of the C 1s is symmetric with respect to the reflection plane of symmetry, and that of O 1s is asymmetric. The O^+ ions are more distributed opposite to the photoelectron. We also extracted the C–O bond length from the diffraction pattern using a simple formula. We found it is tricky to extract the ground state bond length of the multi-atomic molecule using the photoelectron diffraction method due to possible delocalization of core hole and preferentially selection

of bond breaking. There is still large room to improve the model, which is expected to be carried out by theoreticians. We are happy to provide our data to those who are interested in.

Acknowledgments. Supported by the National Natural Science Foundation of China (Grant No. 11574020). The experiment was performed at the PLEIADES beamline at the SOLEIL Synchrotron, France (Grant No. 20130821). We are grateful to E. Robert for technical assistance and to the SOLEIL staff for stable operation of the equipment and the storage ring during the experiments.

References

[1] Yang J *et al.* 2018 *Science* **361** 64
[2] Wang L *et al.* 2018 *Nano Lett.* **18** 5172
[3] Glownia J *et al.* 2016 *Phys. Rev. Lett.* **117** 153003
[4] Itatani J *et al.* 2004 *Nature* **432** 867
[5] Erk B *et al.* 2014 *Science* **345** 288
[6] Wolter B *et al.* 2016 *Science* **354** 308
[7] Liu X J *et al.* 2008 *Phys. Rev. Lett.* **101** 023001
[8] Lucchese R R *et al.* 2012 *J. Phys. B At. Mol. Opt. Phys.* **45** 190201
[9] Kazama M *et al.* 2012 *J. Electron. Spectrosc. Relat. Phenom.* **185** 535
[10] Williams J B *et al.* 2012 *Phys. Rev. Lett.* **108** 233002
[11] Fukuzawa H *et al.* 2019 *J. Chem. Phys.* **150** 174306
[12] Adachi J I *et al.* 2009 *J. Phys. Conf. Ser.* **190** 012049
[13] Lucchese R R *et al.* 2007 *J. Electron. Spectrosc. Relat. Phenom.* **155** 95
[14] Tsuru S *et al.* 2014 *Chem. Phys. Lett.* **608** 152
[15] Saito N *et al.* 2005 *J. Phys. B:* **38** L277
[16] Liu X J *et al.* 2007 *J. Phys. B At. Mol. Opt. Phys.* **40** 485
[17] Landers A *et al.* 2001 *Phys. Rev. Lett.* **87** 013002
[18] Fadley C *et al.* 1997 *Prog. Surf. Sci.* **54** 341
[19] Wider J *et al.* 2001 *Phys. Rev. Lett.* **86** 2337
[20] Fadley C S 1992 *The study of Surface Structures by Photoelectron Diffraction and Auger Electron Diffraction* (Boston, MA: Springer) pp 421–518
[21] Kawai J *et al.* 2008 *Surf. Interface Anal.* **40** 1579
[22] Nakajima K *et al.* 2015 *Sci. Rep.* **5** 14065
[23] Kastirke G *et al.* 2020 *Phys. Rev. X* **10** 021052
[24] Grundmann S *et al.* 2020 *Science* **370** 339
[25] Akoury D *et al.* 2007 *Science* **318** 949
[26] Tsuru S *et al.* 2014 *J. Phys. B:* **47** 071002
[27] Song S *et al.* 2019 *Phys. Rev. A* **99** 022511
[28] Miron C and Morin P 2009 *Nucl. Instrum. Methods Phys. Res. Sect. A Accel. Spectrometers Detectors Associated Equipment* **601** 66
[29] Miron C *et al.* 1997 *Rev. Sci. Instrum.* **68** 3728
[30] Le G K *et al.* 2002 *Rev. Sci. Instrum.* **73** 3885
[31] Liu X J, Nicolas C and Miron C 2013 *Rev. Sci. Instrum.* **84** 033105
[32] Prümper G and Ueda K 2007 *Nucl. Instrum. Methods Phys. Res. Sect. A* **574** 350
[33] Neeb M *et al.* 1998 *J. Electron. Spectrosc. Relat. Phenom.* **88-91** 19
[34] Miyabe S *et al.* 2009 *Phys. Rev. A* **79** 053401
[35] Domcke W and Cederbaum L S 1977 *Chem. Phys.* **25** 189
[36] Kivimäki A *et al.* 1997 *Phys. Rev. Lett.* **79** 998
[37] Hatamoto T *et al.* 2007 *J. Electron. Spectrosc. Relat. Phenom.* **155** 54